Sensors and Actuators A 235 (2015) 227–233

Contents lists available at ScienceDirect

Sensors and Actuators A: Physical

journal homepage: www.elsevier.com/locate/sna

Passive interferometric interrogation of a magnetic field sensor using an erbium doped fiber optic laser with magnetostrictive transducer

I.M. Nascimento[a,b,*], J.M. Baptista[a,c], P.A.S. Jorge[a,b], J.L. Cruz[d], M.V. Andrés[d]

[a] INESC TEC, Rua do Campo Alegre, 687, 4169-007 Porto, Portugal
[b] Department of Physics and Astronomy, Faculty of Sciences of University of Porto, Rua do Campo Alegre 687, 4169-007 Porto, Portugal
[c] Centro de Competências de Ciências Exatas e de Engenharia, Universidade da Madeira, Funchal, Portugal
[d] Department of Applied Physics and Electromagnetism, University of Valencia, Spain

ARTICLE INFO

Article history:
Received 4 March 2015
Received in revised form 20 August 2015
Accepted 8 October 2015
Available online 22 October 2015

Keywords:
Magnetic field sensor
Passive interferometer
Virtual instrumentation
Magnetostrictive material
Erbium doped fiber
Fiber optic laser

ABSTRACT

An erbium doped (Er^{3+}) fiber optic laser is proposed for magnetic field measurement. A pair of FBGs glued onto a magnetostrictive material (Terfenol-D rod) modulates the laser wavelength operation when subject to a static or a time dependent magnetic field. A passive interferometer is employed to measure the laser wavelength changes due to the applied magnetic field. A data acquisition hardware and a LabVIEW software measure three phase-shifted signals at the output coupler of the interferometer and process them using two distinct demodulation algorithms. Results show that sensitivity to varying magnetic fields can be tuned by introducing a biasing magnetic field. A maximum error of 0.79% was found, for magnetic fields higher than 2.26 mT_{RMS}.

1. Introduction

Fiber optic magnetic field sensors have been studied over the years. Special interest has been shown in the high power industry owing to its intrinsic insulation (silica), immunity to electromagnetic interference, high dynamic range and bandwidth and possibility to employ remote interrogation [1]. Several sensing mechanisms such as magnetic fluid, Lorentz force, Faraday effect and magnetostrictive effect have been proposed for magnetic field measurement. These methods can be used with both constant and varying magnetic fields.

The first mechanism was explored by combining the magnetic fluid with an optical fiber refractive index sensor. In the presence of the magnetic field the refractive index of the fluid changes 3×10^{-4} RIU/mT (RIU—Refractive Index Units) at 28 °C from 0 to 70 mT [2].

Sensors established on the Lorentz force require another current carrying conductor (few milliamps) that will experience deformation in the presence of an orthogonal magnetic field. Although they do not experience hysteresis, the deformation induced is very small; in [3] the optical sensor is a Distributed feedback laser, with a Pi-Shift FBG written in Er^{3+} fiber, and the wavelength changes are read with a Michelson interferometer with 25 m of optical path imbalance. A minimal detected field of 1.5 $\mu T/Hz^{1/2}$ was calculated. Another alternative reported consists on using a 6 cm long cavity laser with one longitudinal mode and two orthogonal polarizations. Measurement of the beat frequency between these two polarizations is proportional to the laser birefringence and changes according to pressure exerted in the cavity due to the Lorentz force. Results showed relatively good linearity for magnetic fields between 4 and 20 mT [4].

Faraday effect is one of the most popular optical sensing mechanisms for magnetic field. It consists of light polarization rotation induced by the magnetic field as it propagates through a sensing medium and its sensitivity depends on the medium Verdet constant. While standard fiber optic can be used as a sensing medium to observe the Faraday effect, the Verdet constant of silica is very small and the wounding of the fiber around the conductor gives rise to linear birefringence, further degrading the sensitivity [5]. A prototype operating at 850 nm and based on a Sagnac configuration was developed and tested where a maximum error of 0.2% was achieved for currents ranging from 300 to 4000 A_{RMS} and temperatures from 40 °C up to 60 °C, satisfying 0.5 class operation [6]. Faraday based sensors are affected by the residual birefringence of standard fibers [7], although this problem has been recently over-

---

* Corresponding author.
E-mail address: ivomac88@gmail.com (I.M. Nascimento).

http://dx.doi.org/10.1016/j.sna.2015.10.021
0924-4247/© 2015 Elsevier B.V. All rights reserved.

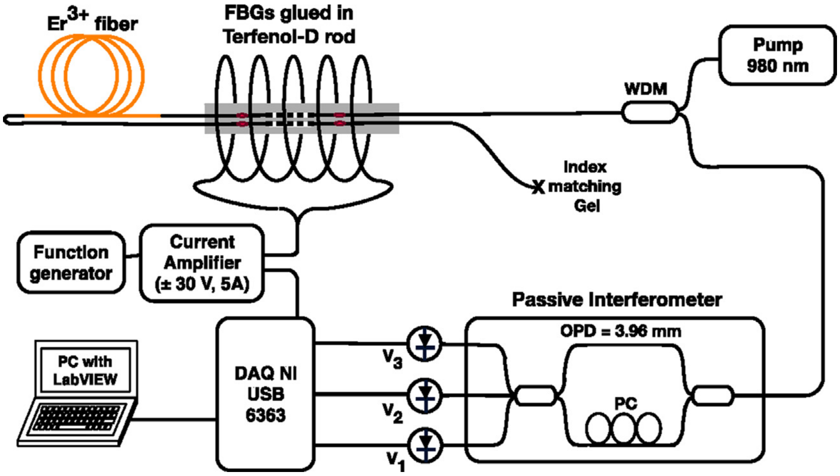

Fig. 1. Experimental setup including the laser, passive interferometer and acquisition setup.

comed in standard fibers [8], an alternative solution has been the use of spun fibers of low birefringence or high circular birefringence [9,10]. On the other hand, the bulk glass materials are more robust and can have higher Verdet constants than fibers. However, fiber alignment with the bulk material is tricky [11,12]. In [11] a sensor operating at 820 nm in a close loop configuration achieved a 5.5% error under stable environmental conditions from 10 A–20 kA.

In the last category, magnetostricitve elements can be deposited or glued to an optical fiber strain sensor. In reference [13], Terfenol-D is deposited in an etched FBG (Fiber Bragg Grating) with 86 μm diameter, improving the sensitivity from 0.386 to 0.95 pm/mT. A distributed sensor was also developed in [14] and consists in wounding a standard single mode fiber around a nickel wire. In the presence of the magnetic field the nickel wire stretches and the phase of the Rayleigh backscattered light changes according to it. A passive Mach–Zehnder interferometer with a 3 × 3 coupler and an OPD of 2 m (1 m spatial resolution) was used to read the phase changes.

In this paper we present an erbium doped optical fiber laser with two FBGs whose wavelength is modulated according to the external magnetic field. The transducer element is a Terfenol-D rod that stretches both FBGs, changing the laser emission wavelength. This variation is converted into an intensity modulation at the output of a passive interferometer using a 3 × 3 output coupler. The laser combines higher SNR (Signal to Noise Ratio) with narrower bandwidth, enabling, together with the interferometric readout system, a higher resolution than is attainable with systems based on the direct modulation of a single FBG.

2. Principle

The implemented setup is demonstrated in Fig. 1. The laser consists of two FBGs at 1534.17 nm with 150 pm spectral width (at half power) and 82% reflectivity, and the other at 1534.21 nm with 160 pm spectral width and 87% reflectivity, written in single mode Boron codoped Photosensitive fiber using a 1058 nm period phase mask. In between the two FBGs, a piece of 6.8 m of Fibercore Erbium doped fiber M-5 is used as the gain medium, resulting in 8 m cavity length.

Each FBG is glued side by side in two points, distant 2 cm apart, in a Terfenol-D (composition $Tb_{0.27}Dy_{0.73}Fe_2$) rod having a diameter of 0.5 cm and 10 cm in length. The thickness of the material limits the magnetic field frequency response to 100 kHz. A function generator, a current amplifier and an inductor are used to generate magnetic field (AC and/or DC with a magnetic-current relation of 12.2 mT/A), modulating both FBGs and consequently the laser wavelength emission. The AC and the DC magnetic field correspond to the alternate and constant field, respectively. Laser operation in reflection is preferable than in transmission as no residual pump power is present in the output.

For the detection of the magnetic field induced wavelength shift, an interferometric readout scheme was set up. A passive interferometer, having a *OPD* of 3.96 mm (Optical Path Difference) resulting in a spectral range of 594 pm between interferometric fringes at 1534 nm was built with a 2 × 2 and a 3 × 3 coupler at the input and output, respectively, producing three outputs with 120 degrees phase difference between them, given by [15]:

$$V_n = A_i + B.\mathrm{Cos}[\varphi(t) + \varphi_{\mathrm{DC}} - (n-1)]\frac{2}{3}\pi \qquad (1)$$

where n is the output 1, 2 and 3, A_i is the DC component obtained when sweeping one period of the interferometer, B is the visibility of the fringes which is maximized by a polarization controller (PC), $\O(t)$ and $\O_{\mathrm{DC}}$ is the time varying and DC interferometer phase, respectively. In such configuration, any change in the laser emission wavelength results in a change of the interferometer optical output phase ($\O(t)$ and $\O_{\mathrm{DC}}$) proportional to the OPD. This way, the interferometer acts like a wavelength-to-intensity modulator enabling to track the wavelength changes, induced by the magnetic field, very accurately with low cost instrumentation.

This interferometer has the advantage of not needing an active element to avoid total output fading. The relative phase of the three outputs and the signal processing can always retrieve the relevant output information, independently of the random drift of the interferometer. Nevertheless, the interferometer drift is mixed with the DC phase changes, also affecting the output intensity and limiting the application of this scheme to AC measurements. In any case, magnetic field measurements were performed in a temperature-controlled environment.

A 16 bits analogue-digital converter from NI (National Instruments) with 305 μV resolution and 2 Mbps bandwidth is used to read the three outputs of the interferometer and the applied current signal to the inductor. In this way, the use of virtual instrumentation becomes possible, making it straightforward to test and implement any signal processing algorithm, by simply adjusting the software, offering a much higher versatility and scalability. Therefore, to test the versatility of virtual instrumentation systems, a LabVIEW program was developed to process the interferometric signals, and used to test and implement, simultaneously, two distinctive demodulation methods. The first one (type I) is presented in Fig. 2 and consists on performing derivatives and an integration as depicted [15]. The output only contains the variant phase infor-